Nucleation of solitary wave complexes in two-component mixture Bose-Einstein condensates

Natalia G. Berloff
Department of Applied Mathematics and Theoretical Physics, Centre for Mathematical Sciences, University of Cambridge, Cambridge, CB3 0WA, United Kingdom
(Dated: 23 December 2004)

Two-component mixtures of Bose-Einstein condensates are shown to support solitary wave complexes that move with a constant velocity preserving their form. I obtain the families of such solitary wave complexes in two-dimensional two-component mixture condensates. These solutions are classified according to the structure of the wavefunction in each component. I show that these complexes nucleate from the surface of the disk when it moves supercritically, therefore, suggesting a mechanism by which these waves can be obtained in condensates by a moving laser beam. The condition for such a nucleation is derived analytically. The flow for supercritical disk velocities is computed numerically. The process of a boundary layer separation with emission of either vortex pairs in each component or a vortex pair in one component and a "slaved wave" in the other component is elucidated.

PACS numbers: 03.75.Lm, 05.45.-a, 67.40.Vs, 67.57.De

The systems of the coupled nonlinear Schrödinger (NLS) equations are fundamental and universal systems that have been used to describe motions in conservative systems of weakly nonlinear dispersive waves in continuum mechanics, plasma physics, nonlinear optics and condensed matter. Recent experimental advances in multi-component Bose-Einstein condensates (BECs) stimulated the interest in solitary wave solutions of these equations and their production as they define the possible excitation states that multi-component BECs can support. Multi-component condensates have been formed by simultaneous trapping and cooling of atoms in distinct spin or hyperfine levels [1]. There is also a hope to obtain condensed mixtures of different atomic species [2]. In this respect a lot of attention has been paid to discovering the topological solitons and defects such as domain walls [3] and skyrmions (vortons) [4] in the regime of phase separation. In the regime where phases do not separate, the complete families of three-dimensional solitary wave solutions were obtained in [5]. There solutions were classified according to the structure of the wavefunction of each component. Four basic types were noted: (1) vortex rings of various radii in each component, (2) a vortex ring in one component coupled to a rarefaction solitary wave of the other component, (3) two coupled rarefaction waves, (4) either a vortex ring or a rarefaction pulse coupled to a localised disturbance of a very low momentum. The continuous families of such waves were shown in the momentum-energy plane for various values of the interaction strengths and the relative differences between the chemical potentials.

Two-dimensional solutions of the coupled NLS equations are relevant in the view of the experimental setting for studies of multi-component BECs, for instance, two-dimensional vortex complexes were shown to nucleate in rotating two-component condensates [6] giving rich equilibrium structures such as triangular, square and double-core lattices and vortex sheets. The goal of this letter is to obtain complete families of solitary wave solutions in two-dimensional two-component mixture BECs and to find the conditions for their creation in bulk condensates.

For two components, described by the wave functions ψ_1 and ψ_2, with N_1 and N_2 particles respectively, the system of the Gross-Pitaevskii (GP) equations (the coupled NLS equations) on the wave functions of the condensate components become

$$\mathrm{i}\hbar\frac{\partial\psi_1}{\partial t} = \left[-\frac{\hbar^2}{2m_1}\nabla^2 + V_{11}|\psi_1|^2 + V_{12}|\psi_2|^2\right]\psi_1, \quad (1)$$

$$\mathrm{i}\hbar\frac{\partial\psi_2}{\partial t} = \left[-\frac{\hbar^2}{2m_2}\nabla^2 + V_{12}|\psi_1|^2 + V_{22}|\psi_2|^2\right]\psi_2, \quad (2)$$

where m_i is the mass of the atom of the ith condensate, and the coupling constants V_{ij} are proportional to scattering lengths a_{ij} via $V_{ij} = 2\pi\hbar^2 a_{ij}/m_{ij}$, where $m_{ij} = m_i m_j/(m_i + m_j)$ is the reduced mass. The interaction conserves the number of atoms of the two species, so $\int |\psi_i|^2\, dxdy = N_i$. To study the equilibrium properties the energy functional has to be minimized subject to constraint on conservation of particles leading to introduction of two chemical potentials $\mu_1 = V_{11}n_1 + V_{12}n_2, \mu_2 = V_{12}n_1 + V_{22}n_2$, where $n_i = |\psi_i|^2$ is the number density in equilibrium. The dispersion relation between the frequency ω and the wave number k of the linear perturbations ($\propto \exp[i\mathbf{k}\cdot\mathbf{x} - i\omega t]$) around homogeneous states is obtained as

$$(\omega^2 - \omega_1^2)(\omega^2 - \omega_1^2) = \omega_{12}^4, \quad (3)$$

where $\omega_i^2(k) = c_i^2k^2 + \hbar^2k^4/4m_i^2$ coincides with a one-component Bogoliubov spectrum with the customary defined sound velocity $c_i^2 = n_iV_{ii}/m_i$ and $\omega_{12}^2 = c_{12}^2k^2$ where $c_{12}^4 = n_1n_2V_{12}^2/m_1m_2$. The system is dynamically stable if the spectrum (3) is real and positive which

implies that $V_{11}V_{22} > V_{12}^2$ for stability. The acoustic branches of Eq. (3) are $\omega_\pm \approx c_\pm k$ with the corresponding sound velocities $2c_\pm^2 = c_1^2 + c_2^2 \pm \sqrt{(c_1^2 - c_2^2)^2 + 4c_{12}^4}$. The solitary waves I seek below are all subsonic, so their velocity U is less than c_-.

Solitary waves. I shall restrict the parameter space by letting $m_1 = m_2 = m$, $V_{11} = V_{22}$, $\alpha = V_{12}/V_{11}$. To find axisymmetric solitary wave solutions moving with the velocity U in the positive $x-$direction, I solve

$$2\mathrm{i}U\frac{\partial\psi_1}{\partial x} = \nabla^2\psi_1 + (1 - |\psi_1|^2 - \alpha|\psi_2|^2)\psi_1 \quad (4)$$

$$2\mathrm{i}U\frac{\partial\psi_2}{\partial x} = \nabla^2\psi_2 + (1 - \alpha|\psi_1|^2 - |\psi_2|^2 - \Lambda^2)\psi_2, \quad (5)$$

$$\psi_1 \to \psi_{1\infty}, \quad \psi_2 \to \psi_{2\infty}, \quad \text{as} \quad |\mathbf{x}| \to \infty,$$

where a dimensionless form of Eqs. (1–2) is used, such that the distances are measured in units of the correlation (healing) length $\xi = \hbar/\sqrt{2m\mu_1}$, the frequencies are measured in units $2\mu_1/\hbar$ and the absolute values of the fields $|\psi_1|^2$ and $|\psi_2|^2$ are measured in units of particle density μ_1/V_{11}. Also present in Eqs. (4–5) is the measure of asymmetry between chemical potentials $\Lambda^2 = (\mu_1 - \mu_2)/\mu_1$ (where we assume that $\mu_1 > \mu_2$). The condition of dynamical stability under which two components do not separate is $\alpha^2 < 1$. The values of the wave-functions of the solitary waves at infinity in Eqs. (4–5) are given by $\psi_{2\infty}^2 = (1 - \alpha - \Lambda^2)/(1 - \alpha^2)$ and $\psi_{1\infty}^2 = 1 - \alpha\psi_{2\infty}^2$ and the critical speed of sound is $4c_\pm^2 = \psi_{1\infty}^2 + \psi_{2\infty}^2 \pm \sqrt{(\psi_{1\infty}^2 - \psi_{2\infty}^2)^2 + 4\alpha^2\psi_{1\infty}^2\psi_{2\infty}^2}$, so that $c_- > 0$ implies $\Lambda^2 < 1 - \alpha$.

To find each solitary wave complex, I will fix α, Λ^2, and U, solve Eqs. (4–5) by Newton-Raphson iteration procedure described in [5] and calculate the momenta $\mathbf{p}_i = \frac{1}{2\mathrm{i}}\int[(\psi_i^* - \psi_{i\infty})\nabla\psi_i - (\psi_i - \psi_{i\infty})\nabla\psi_i^*]\,dxdy$ and energy

$$\mathcal{E} = \frac{1}{2}\int\sum_{i=1}^{2}\{|\nabla\psi_i|^2 + \frac{1}{2}(\psi_{i\infty}^2 - |\psi_i|^2)^2\}\,dxdy + \frac{\alpha}{2}\int\prod_{i=1}^{2}(\psi_{i\infty}^2 - |\psi_i|^2)\,dxdy \quad (6)$$

per unit length in z-direction. Similarly to the three-dimensional case [5] we can show that $U = \partial\mathcal{E}/\sum p_i$ where the derivative is taken along the solitary wave sequence. Also, we multiply Eqs. (4–5) by $x\partial\psi_i^*/\partial x$ and their complex conjugates by $x\partial\psi_i/\partial x$, integrate by parts over all space, and compare the result with (6) which gives $\mathcal{E} = \int\sum|\partial\psi_i/\partial x|^2\,dxdy$. Similarly, firstly we replace ψ_i by $\psi_i - \psi_{i\infty}$ in the first term of the first integral of Eq. (6) and integrate by parts, secondly we multiply Eqs. (4–5) by $y\partial\psi_i^*/\partial y$ and integrate by parts which gives us two more integral properties that will be used as checks of the numerical work

FIG. 1: (colour online) The dispersion curves of several families of the solitary wave solutions of Eqs. (4–5). The solid lines show three families of solutions with $\alpha = 0.5$ and $\Lambda^2 = 0.1$. The numbers next to the dots give the velocity of the solitary wave. The top (black) branch corresponds to VP-VP complexes. The middle (green) branch shows p vs $\mathcal{E}$ for VP-SW complexes and the bottom (red) branch is the dispersion curve of SW-VP complexes. The dashed (blue) line across the solid black branch shows the VP-VP complexes for $U = 0.2$, $\Lambda^2 = 0.1$ as the intercoupling parameter α increases in increments of 0.1 from 0.1 (top point) to 0.7 (bottom point). The light grey (magenta) dashed line shows the VP-VP complexes for $U = 0.2$ and $\alpha = 0.5$ with the asymmetry parameter Λ^2 taking values 0.05 (top point), $0.1, 0.2, 0.3$ (bottom point). The insets show the plots of $z = |\psi_1(x,y)|^2$ (top) and $z = |\psi_2(x,y)|^2$ (bottom) for the VP-SW complex with $U = 0.2$, $\alpha = 0.5$, $\Lambda^2 = 0.1$.

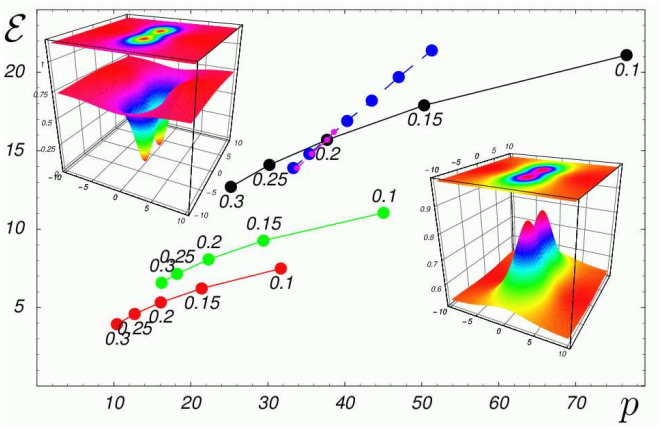

$$U\sum p_i = \frac{1}{2}\int\sum(\psi_{i\infty}^2 - |\psi_i|^2)^2 dxdy + \alpha\int\prod(\psi_{i\infty}^2 - |\psi_i|^2)\,dxdy, \quad (7)$$

$$\mathcal{E} = \frac{1}{4}\int(1 - |\psi_1|^2 - \alpha|\psi_2|^2) \times(3\psi_{1\infty}^2 - \psi_{1\infty}(\psi_1 + \psi_1^*) - |\psi_1|^2)\,dxdy + \frac{1}{4}\int(1 - \alpha|\psi_1|^2 - |\psi_2|^2) \times(3\psi_{2\infty}^2 - \psi_{2\infty}(\psi_2 + \psi_2^*) - |\psi_2|^2)\,dxdy. \quad (8)$$

In the limit $\alpha \to 0$, two components become uncoupled, in which case the solitary wave sequence for each component follows the dispersion curve of the one-component GP equation calculated in [7]. The family of solitary waves in 2D is represented by a pair of point vortices (VP) of opposite circulation if $U_c < 0.56c_i$. These vortices are separated by distance $2b_i \sim U^{-1}$ for small U. As the velocity increases, the wave loses its vorticity and becomes a rarefaction pulse (RP). As $U \to c_i$ both energy and momentum per unit length approach zero and

the solutions asymptotically approach the 2D rational solution of Kadomtsev-Petviashvili Type I equation. The sequence merges tangentially with the phonon branch of the dispersion curve in each of the uncoupled components. For $\alpha \neq 0$ $c_1 \neq c_2$, so different components become RP at different critical values of U and a variety of complexes becomes possible. Table 1 gives an example of various transitions from one complex to another as the velocity U increases in the system with $\alpha = 0.05$ and $\Lambda^2 = 0.1$.

Table 1. The velocity, U, energy, $\mathcal{E}$, momenta, p_i, and half-separations between centres of the point vortices, b_i, of the solitary wave solutions of Eqs. (4–5) with $\alpha = 0.05$ and $\Lambda^2 = 0.1$. The sequence terminates at $U = c_- \approx 0.646$.

U	$\mathcal{E}$	p_1	p_2	b_1	b_2	complex
0.40	14.7	13.8	12.1	0.915	0.498	VP-VP
0.43	13.7	12.5	10.9	0.184	–	VP-RP
0.45	13.0	11.7	10.2	–	–	RP-RP
0.5	11.4	9.90	8.46	–	–	RP-RP
0.6	7.68	6.29	5.36	–	–	RP-RP

Next I will consider the cases of more intermediate values of intercoupling interaction strength. In addition to the VP-VP, VP-RP, and RP-RP complexes, there are new classes of solitary waves that have no analog in one-component condensates. In these complexes the disturbance of a very low impulse in one condensate (called "slaved wave" (SW)) is dragged by either VP or RP structure of the other component. The density of SW is maximal where the density of either VP or RP is minimal and vise versa. For fixed values of α and Λ^2 the system has three families of solitary wave complexes: VP(RP)-VP(RP), SW-VP(RP) and VP(RP)-SW as Fig.1 illustrates. Also, Fig.1 shows the dispersion curves of several other families of the solitary wave solutions in the system when two out of three parameters (α, Λ^2 and U) are kept fixed.

Nucleation. In a pioneering paper Frisch et al. [8] used a direct numerical simulation of the one-component GP equation to show that the superflow around a disk releases vortices from the perimeter of the disk creating a net drag force beyond a critical velocity. The criteria for vortex nucleation was related to the transonic transition, namely, the vortices are created when the local speed of sound is reached somewhere in the mainstream. The argument supporting this conclusion is based on the observation that the hydrodynamical form of the steady state one component GP equation away from the disk boundary changes its type from being elliptic to hyperbolic if the local speed of sound is exceeded. One would expect that somewhat similar scenario should exist for vortex nucleation in multi-component condensates. But in two-component condensates there are several sound speeds: c_1, c_2, c_{12}, c_- and c_+. So which of these values leads to vortex nucleation? The argument based on the criterion of the dynamical stability that the vortices should nucleate as soon as the flow reaches the local c_- value can be refuted by the reference to a one-component GP equation with a nonlocal potential that allows for the roton minimum in the dispersion curve [9] and therefore has two critical velocities: speed of sound c and the Landau critical velocity v_L, $v_L < c$. We have shown in [9] that the nucleation of vortices is related to c and not to v_L. Another difficulty is that in multi-component condensates each component has its own velocity $\mathbf{u}_i$. Will vortices nucleate when the velocity of just one component reaches the criticality or is there a more intrinsic relationship between the velocities of the components and critical velocity? Finally, as we discovered above there exist more than one vortex complex, so which complex nucleates at the criticality? Next I answer these questions using a simple analytical argument and direct numerical simulations.

By using the Madelung transformations $\psi_i = R_i \exp[\mathrm{i}S_i]$ in Eqs. (1–2) and separating the real and imaginary parts, one gets the following hydrodynamical equations for the number density $n_i = R_i^2$ and the phase $\phi_i = \hbar S_i/m$ for the superflow with $\phi_i = u_\infty x$ as $x^2 + y^2 \to \infty$

$$\frac{\partial n_i}{\partial t} + \nabla \cdot (n_i \nabla \phi_i) = 0 \tag{9}$$

$$\frac{\partial \phi_i}{\partial t} + \frac{1}{2}|\nabla \phi_i|^2 - \frac{1}{2}u_\infty^2 + \frac{V_{ii}}{m_i}(n_i - n_{i\infty}) + \frac{V_{12}}{m_i}(n_j - n_{j\infty}) = \frac{\hbar^2}{2m_i^2}\frac{\nabla^2 n_i^{1/2}}{n_i^{1/2}}, \tag{10}$$

where $j = 2$ if $i = 1$ and $j = 1$ if $i = 2$. We consider a stationary flow and neglect the quantum pressure terms on the right hand side of Eq. (10) due to our interest in mainstream flow. Since two components are coupled through their amplitudes, the velocity vectors of two components are parallel. We fix a point outside of the disk at which the components move with velocities $\mathbf{u}_i$, introduce the local orthogonal coordinates such that the $x-$axis is tangent to the flow and expand ϕ_i in the neighbourhood of this point as $\phi_i \approx u_i x + \epsilon\tilde{\phi}_i$, where ϵ is a small parameter. To the leading order Eqs. (9-10) become

$$A\tilde{\phi}_{ixxxx} + B\tilde{\phi}_{ixxyy} + C\tilde{\phi}_{iyyyy} = 0, \tag{11}$$

where $A = \partial(n_1u_1)/\partial u_1 \times \partial(n_2u_2)/\partial u_2 - u_1u_2\partial n_1/\partial u_2 \times \partial n_2/\partial u_1$, $B = n_2\partial(n_1u_1)/\partial u_1 + n_1\partial(n_2u_2)/\partial u_2$ and $C = n_1n_2$ where now $n_i = n_i(u_1, u_2)$. Note, that $B^2 \geq 4AC$ for all u_i, therefore, Eq. (11) is elliptic (in the sense that it has no real characteristics $\partial\tilde{\phi}_i/\partial y + \lambda\partial\tilde{\phi}_i/\partial x = 0$) if and only if $A > 0$. This gives the criterion for the vortex nucleation: the boundary layer separation with

nucleation of vortices takes place when

$$\frac{\partial(n_1u_1)}{\partial u_1}\frac{\partial(n_2u_2)}{\partial u_2} = u_1u_2\frac{\partial n_1}{\partial u_2}\frac{\partial n_2}{\partial u_1}, \qquad (12)$$

somewhere in the mainstream. In our special case of equal masses and intracomponent coupling parameters, condition (12) in dimensionless units becomes

$$(n_1 - 2u_1^2)(n_2 - 2u_2^2) = 4\alpha^2 n_1^2 n_2^2. \qquad (13)$$

Note that if $\alpha = 0$, then the criterion (13) says that the criticality occurs when the mainstream velocity reaches the local speed of sound $2u_c = n_c$. If $\alpha \neq 0$ and if at criticality $u_1 \approx u_2 = u_c$, then $u_c = c_{l-}$, where c_{l-} is a *local* speed of sound defined by $4c_{l-}^2 = n_1 + n_2 - \sqrt{(n_1 - n_2)^2 + 4\alpha^2 n_1 n_2}$, but in general Eq. (13) can be satisfied when u_1 and u_2 bracket c_{l-}.

Direct numerical simulations of Eqs. (1–2), with $-2i\psi_{it}$ added to the left hand sides and in the frame of reference in which the disk is stationary so $U = u_\infty$, show vortex complex nucleation in supercritical flow around the disk. This suggests that these complexes could be generated by a laser beam which moves supercritically in trapped condensates. At subcritical velocity ($U < 0.225$), the flows of the condensates are symmetric fore and aft of the direction of motion, and the disk experiences no drag. When the condition (13) is satisfied, which happens first on the disk equator where the velocities are maximal, the condensates evade shocks through a boundary layer separation. Fig. 2 shows the emission of various complexes for the disk of the radius 10 healing lengths that moves with supercritical velocity $U = 0.28$. The disk sheds SW-VP, VP-SW and VP-VP complexes in the order and frequency that depends on the value of the disk's velocity. These complexes move more slowly than the disk and form a vortex wave street that trails behind it, maintained by other complexes that the disk sheds. As the velocity of the disk increases such a shedding becomes more and more irregular. Each complex is born at one particular latitude within the healing layer on the disk. As it breaks away into the mainstream, it at first contributes a flow that depresses the mainstream velocities on the disk below critical. For larger values of the disk velocity ($U > 0.265$), more energy is required for this depression and VP-VP complex that has larger energy than SW-VP complexes is born first. At low supercritical velocities SW-VP complex is born first. As it moves further downstream however, its influence on the surface flow diminishes. The surface flow increases until it again reaches criticality, when a new complex is nucleated and the whole sequence is repeated. The vortex and slaved wave street trailing behind the disk creates a drag on the disk that decreases as the nearest complex moves downstream, but which is refreshed when a new complex is born. The complexes downstream of the disk move with different velocities and interact among themselves. These interactions may lead to a transformation from one type of the complex to another; Fig. 2 shows the splitting of the VP-VP complex into SW-VP and VP-SW complexes. The mechanism in which solitary waves transfer energy from one to another was elucidated in [10] for a one-component condensate.

FIG. 2: (colour online) The time snapshots of $|\psi_1|^2$ (top) and $|\psi_2|^2$ (bottom) of the solution of Eqs. (4–5) with $-2i\psi_{it}$ added to the left hand sides with $\alpha = 0.5$, $\Lambda^2 = 0.1$ for the flow around a disk of radius 10 moving to the right with velocity $U = 0.28$. The solitary wave street is seen in the wake of the disk. The complexes were emitted in the order VP-VP, SW-VP, VP-SW, and SW-VP complex has just got emitted from the disk boundary. For this large supercritical velocity the VP-VP complex is first nucleated from the surface of the disk and the insets show this moment at an earlier time. On the main panels this complex is in the process of splitting into the VP-SW and SW-VP complexes. Only parts of the computational box are shown.

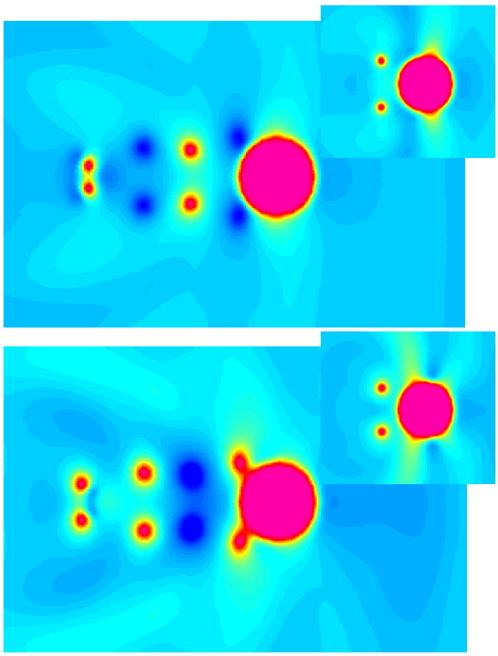

The support from NSF grant DMS-0104288 is acknowledged.

[1] C.J.Myatt *et al.*, Phys. Rev. Lett., **78**, 586 (1997); D.S.Hall *et al.,* Phys. Rev. Lett., **81**, 1539 (1998); D.M. Stamper-Kurn *et al.,* Phys. Rev. Lett., **80**, 2027 (1998); J. Stenger *et al.,* Nature (London), **396**, 345 (1998).

[2] G.Modugno *et al.*, Science, **294**, 1320 (1998); M. Mudrich *et al.,* Phys. Rev. Lett. **88**, 253001, (2002).

[3] S. Coen and M. Haelterman, Phys. Rev. Lett., **87**, 140401 (2001).

[4] J.Ruostekoski and J.R.Anglin, Phys. Rev. Lett., **86**, 3934 (2001); C.M.Savage and J.Ruostekoski, Phys. Rev.

Lett., **91**, 010403 (2003); R.A.Battye, N.R. Cooper and P.M. Sutcliffe, Phys. Rev. Lett., **88**, 080401 (2002)
[5] N.G. Berloff cond-mat/0412099.
[6] K. Kasamatsu, M. Tsubota and M. Ueda, Phys. Rev. Lett., **91**, 150406 (2003); K. Kasamatsu, M. Tsubota and M. Ueda, Phys. Rev. Lett., **93**, 250406 (2004).
[7] C. A. Jones and P. H. Roberts, J. Phys. A **15** 2599 (1982); C. A. Jones, S. J. Putterman, and P. H. Roberts, J. Phys. A: Math. Gen. **19** 2991 (1986)
[8] T. Frisch, Y. Pomeau and S. Rica, Phys. Rev. Lett., **69**, 1644 (1992)
[9] N.G. Berloff and P.H. Roberts, Phys. Letts. A, 274, 69-74(2000)
[10] N.G. Berloff, J. Phys. A, **37**, 1617 (2004)